Progress In Electromagnetics Research M, Vol. 107, 13–23, 2022

A Triple Band Highly Sensitive Refractive Index Sensor Using Terahertz Metamaterial Perfect Absorber

Sagnik Banerjee[1], Purba Dutta[1], Amitkumar V. Jha[1], Prabhat R. Tripathi[2], Avireni Srinivasulu[3], Bhargav Appasani[1, *], and Cristian Ravariu[4]

Abstract—This research introduces a novel design of a metamaterial absorber having the range in terahertz, capable of sensing changes in the refractive index of the encircling medium. The layout includes adjoining rectangular patches in the form of a plus symbol along with four circular patch resonators (CPRs) on the pinnacle of a Gallium Arsenide (GaAs) substrate. The proposed design comes up with three consecutive absorption peaks, with an absorptivity of 99.0%, 99.75%, and 98.0% at three different resonant frequencies of 2.36 THz, 2.675 THz, and 2.97 THz, respectively, and a Full Width Half Maximum (FWHM) of 0.08, 0.04, and 0.05. This structure's quality factor (Q-factor) at the three resonant frequencies is 29.5, 66.8, and 59.4 together with 6.75, 17.5, and 30 as figure of merit (FoM), respectively. The proposed design offers a sensitivity of 0.54 THz/RIU, 0.7 THz/RIU, and 1.5 THz/RIU in those three absorption bands. To support the selection of design parameters, parametric assessment was done. The designed sensor can find its applications in terahertz sensing.

1. INTRODUCTION

Metamaterials, composed of periodic sub-wavelength or deep-sub-wavelength structures, are artificially architectured composite structures that exhibit distinctive properties like permeability, refractive index, negative permittivity, optical magnetism, etc. Due to their exclusive properties, realized by physical means rather than chemical composition, these structures have attracted many researchers [1]. One of the subclasses of the structures, which absorbs the electromagnetic radiation incident upon them, is called metamaterial absorber. Due to its various applications, it has become a vital area of research [2]. A unique design of multiband metamaterial absorber operating in the 5–12 GHz frequency range has been reported in [3]. Another triple band metamaterial absorber based on hexagonal Split Ring Resonators (SRRs) was reported in [4] for detecting fuel contamination. A double band chiral metamaterial absorber was proposed in [5] to decide the standard of car lubricants in the MHz frequency regime. Another metamaterial absorber was proposed in [6] for X-band applications. These absorbers operate in the GHz and MHz frequency regimes. Metamaterial absorbers in the terahertz regime can be created with proper scaling and by proper choice of design materials [7, 8]. Terahertz metamaterial absorbers (TMA) can also function as extremely high-quality sensors [9, 10]. A silicon nitride-based bio-sensor was designed to estimate the thickness of thin films having a sensitivity of 4.05×10^{-2} GHz/nm [11]. Similarly, sensors were developed for measuring temperature in which the absorption spectra shift with the variations in the temperature [12]. Bio-sensing applications have been achieved using TMAs that provided frequency shifts as 275 GHz [13] and 3.6 GHz [14]. TMAs are also

Received 7 October 2021, Accepted 22 December 2021, Scheduled 30 December 2021

* Corresponding author: Bhargav Appasani (bhargav.appasanifet@kiit.ac.in).

[1] School of Electronics Engineering, Kalinga Institute of Industrial Technology, Bhubaneswar, India. [2] Department of Electronics and Electrical Engineering, Birla Institute of Technology, Mesra, India. [3] School of Engineering & Technology, K. R. Mangalam University, Gurugram-122103, India. [4] Department of Electronic Devices, Circuits and Architectures, Polytechnic University of Bucharest, Bucharest, Romania.

used to determine the refractive index of the surrounding medium. A single band TMA for refractive index sensing applications was developed, with a sensitivity of 300 GHz per refractive index unit (RIU), a Q-factor of 22.5, and a figure of merit (FoM) of 2.94 [15]. Another single band TMA was proposed in [16] that could detect the changes in the surrounding medium's refractive index with a sensitivity of 1.5 THz/RIU. Another refractive index sensor was introduced based on a defective square ring resonator on the top of Teflon dielectric spacer in [17], having a sensitivity of 300 GHz/RIU. It is necessary to considerably limit the resonance bandwidth while designing a high Q-factor sensor. Designs with a high Q-factor are sensitive and serve well as sensors. Table 1 outlines numerous designs presented by researchers for employing TMAs to measure the refractive index of the surrounding medium.

Table 1. Sensing performance comparison.

Ref. No.	No of absorption bands	Sensitivities (GHz/RIU)	Resolution (RIU)
[18]	1	135	0.2
[19]	1	147	0.02
[20]	1	187	0.1
[21]	1	851	0.1
[22]	1	139.2	0.2
[23]	1	0.3537	0.5
[24]	1	1317	0.02
[25]	1	105	0.2
[26]	2	638, 582	0.2
[27]	2	280.8, 201.6	0.1
[28]	2	470, 760	0.01
[29]	3	72, 103.5, 139.5	0.2
[30]	3	57.5, 152.5, 51.4	0.2
[31]	3	1600, 300, 200	0.02
This paper	3	540, 700, 1500	0.01

In recent times, researchers are more interested in designing multi-band absorbers due to its applications in the field of multi-spectral sensing and detection [29–31]. But the drawback is that these multi-band sensors could not perform equally well in all the absorption bands. An efficient multi-band metamaterial absorber that exhibits good sensing characteristics in all the absorption bands has to be designed. In this paper, an exclusive design of a refractive index sensor has been proposed in the terahertz frequency regime. The design incorporates gold metal on top of a Gallium Arsenide (GaAs) substrate. The design's absorption peaks move with differences in the refractive index of the encompassing medium and have a resolution of 0.01 RIU. The design finds three absorption bands with peak absorptions of 99.0%, 99.75%, and 98.0% at 2.36 THz, 2.675 THz, and 2.97 THz, respectively. The full width half maximum (FWHM) for the absorption peaks has been found to be 0.08, 0.04, and 0.05, with the corresponding quality factor (Q factor) of 29.5, 66.8, and 59.4. The corresponding sensitivities are calculated to be 0.54 THz/RIU, 0.7 THz/RIU, and 1.5 THz/RIU, and the respective FoM is 6.75, 17.5, and 30.

The paper has the following sections. The structural architecture of the suggested sensor is shown in the next section. The simulation results are provided in the third section, along with a description of the process underlying the emergence of the absorption peaks using current distribution plots. In addition, parametric analysis of the design parameters is performed to support the selection of design parameters. This section also yields the sensitivities of the various absorption bands. Finally, the final portion offers the work's conclusion.

2. PROPOSED SENSOR

The unit cell design of the terahertz metamaterial absorber has been presented in Fig. 1. Gold has been used on the top surface along with bottom plane of the structure as its oscillation frequency of 6.5 THz falls within the THz spectrum [32], and its conductivity is 4.10×10^7 S/m. Gallium Arsenide (GaAs), a compound semiconductor, is used as a dielectric spacer due to its wide band gap and high resistivity, possessing a permittivity of 12.94 and loss tangent of 0.006. The height of the unit cell is given as $h = 5\,\mu$m. Thickness of the top layer is introduced as $b = 0.4\,\mu$m, which contains adjoining rectangular patches in the form of a plus symbol and four Circular Patch Resonators (CPRs), with each of the radius $r = 13\,\mu$m situated near the corner of the unit cell. The designed absorber experiences fine mechanical flexibility due to its lower substrate height, which makes it suitable for multiple applications in the terahertz regime. Thickness $t = 2\,\mu$m has been taken for the backside Gold layer to prevent the electromagnetic wave transmission. The length unit cell is denoted as $u = 100\,\mu$m. Therefore, the recommended geometric specifications for the design are: $u = 100\,\mu$m, $r = 13\,\mu$m, $t = 2\,\mu$m, $a = 6\,\mu$m, $b = 0.4\,\mu$m, and $h = 5\,\mu$m. On the unit cell's sides, periodic boundary conditions are imposed. Transverse Electromagnetic wave (TEM) is incident on structure along the z axis.

Figure 1. Design of terahertz metamaterial absorber: (a) top view; (b) side view.

3. ABSORPTION CHARACTERISTICS

The CST Microwave Studio software was used for the structure's design and simulation. The structure's absorption is determined by Equation (1).

$$A_x = 1 - R_x - T_x \tag{1}$$

where A_x is the absorption coefficient, T_x the coefficient of transmission, and R_x the coefficient of reflection. T_x is taken as zero as the electromagnetic wave transmission is not permitted by the thick ground metal plane, whose thickness is taken greater than the skin depth of gold. The absorption spectrum of the designed metamaterial absorber is shown in Fig. 2. The resonance frequencies are at 2.36 THz (band 1), 2.675 THz (band 2) and 2.97 THz (band 3) with near perfect absorption of 99.0%, 99.75%, and 98.0%, respectively.

The absorption characteristics of the sensor do not significantly change with the variations in the polarization angle up to 30°. Because of the narrow absorption bandwidth, the design's FWHMs are 0.08 THz, 0.04 THz, and 0.05 THz, resulting in high-frequency selectivity. Furthermore, the Q factor of the design, which is the ratio of the resonant frequency to the FWHM, is determined to be 29.5, 66.8, and 59.4 for the three separate absorption peaks, respectively.

The impedance is plotted as a function of frequency as shown in Fig. 3. From the plot it is clear that maximum absorption occurs when the real part of the impedance is matching with that of the free space, and the imaginary part of the impedance is close to zero. The impedance matching occurs at the three resonance frequencies of 2.36 THz, 2.675 THz, and 2.97 THz.

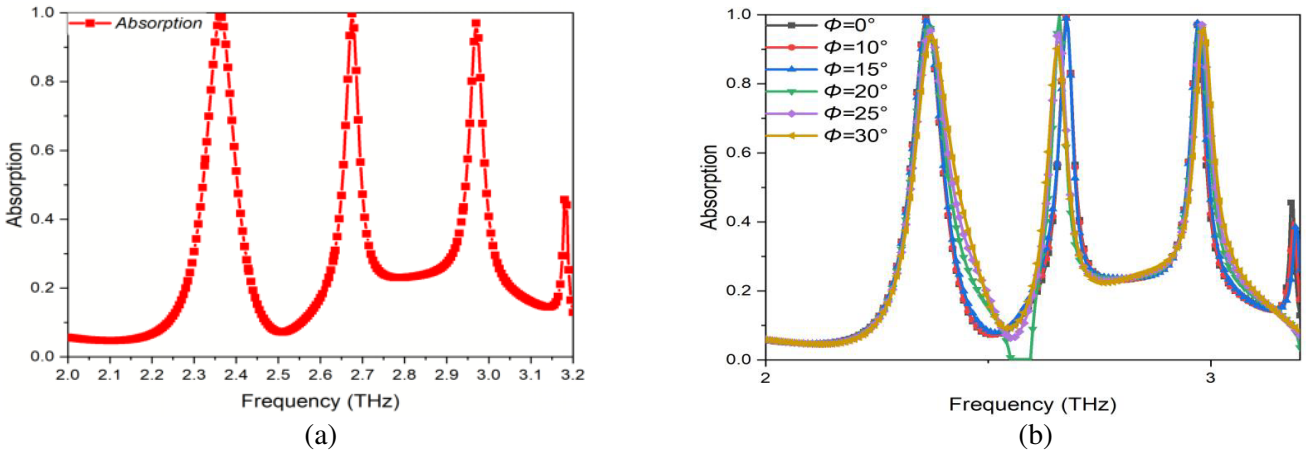

Figure 2. (a) Absorption characteristics. (b) Absorption vs polarization angle.

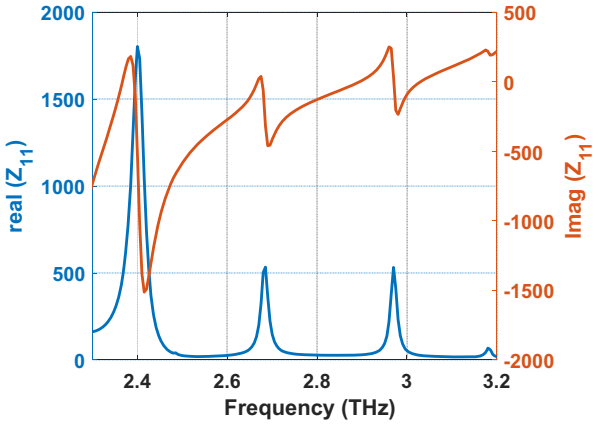

Figure 3. Impedance of the proposed structure.

The real parts of the effective permittivity and effective permeability are also obtained for the given unit cell dimension of $u = 100\,\mu m$ and are shown in Fig. 4. It can be seen that absorption takes place when the real part of the permittivity is negative, and the real part of the permeability is positive. Thus, the designed structure acts as a single negative (SNG) metamaterials. Especially, as its permittivity is negative and its permeability positive, it is an epsilon negative (ENG) metamaterial, and the resonance is plasmonic in nature.

For better understanding of the absorption mechanism, the surface current distribution at three different resonant frequencies has been depicted in Fig. 5. Fig. 5(a) represents the distribution of surface current at 2.36 THz. It is clearly observed that the current is concentrated along the x axis of the plus sign, indicating that the resonance at this frequency is due to the horizontal rectangular patch of the plus sign. Fig. 5(b) portrays the distribution of surface current at 2.675 THz. Here, the current concentration is concentrated on the vertical rectangular patch along the y-axis and also due to the four CPRs. Hence, it can be said that the resonance at this frequency is due to CPRs as well as the vertical rectangular patch. Fig. 5(c) shows the surface current distribution at 2.97 THz. It is seen that the current is weakly distributed over the entire top plane, including the metallic as well as dielectric regions.

For justifying the design parameters, a parametric sweep is carried out. Fig. 6 shows the parametric analysis for the height or thickness of the substrate (h) at three distinct resonant frequencies, and it is apparent that as the height of the substrate grows, so does the resonant frequency, and vice versa. From Fig. 6(a), it is observed that a maximum absorption, with a narrower FWHM resulting in higher

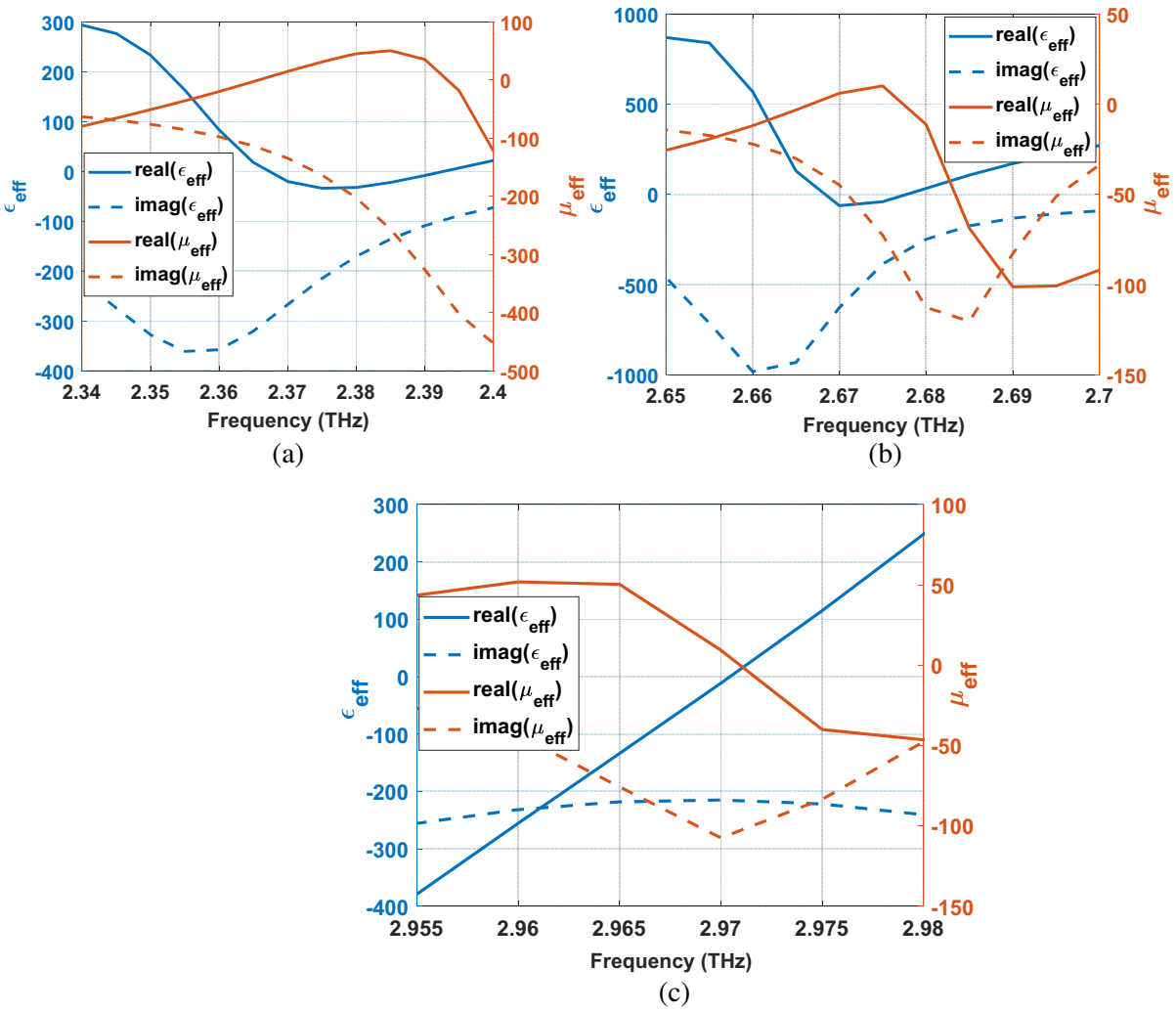

Figure 4. Effective permeability and effective permeability for (a) 2.36 THz, (b) 2.675 THz, (c) 2.97 THz.

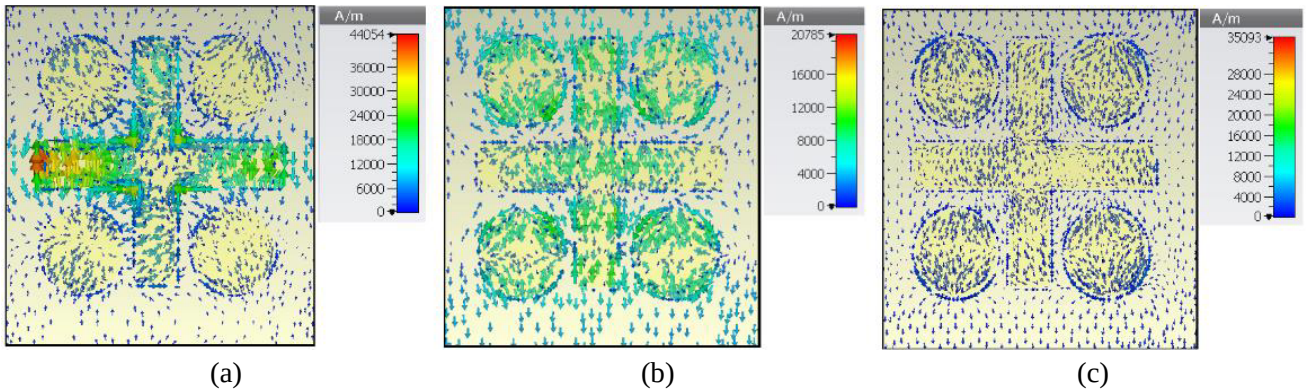

Figure 5. Surface current distribution for the proposed TMA at (a) 2.36 THz, (b) 2.675 THz, (c) 2.97 THz.

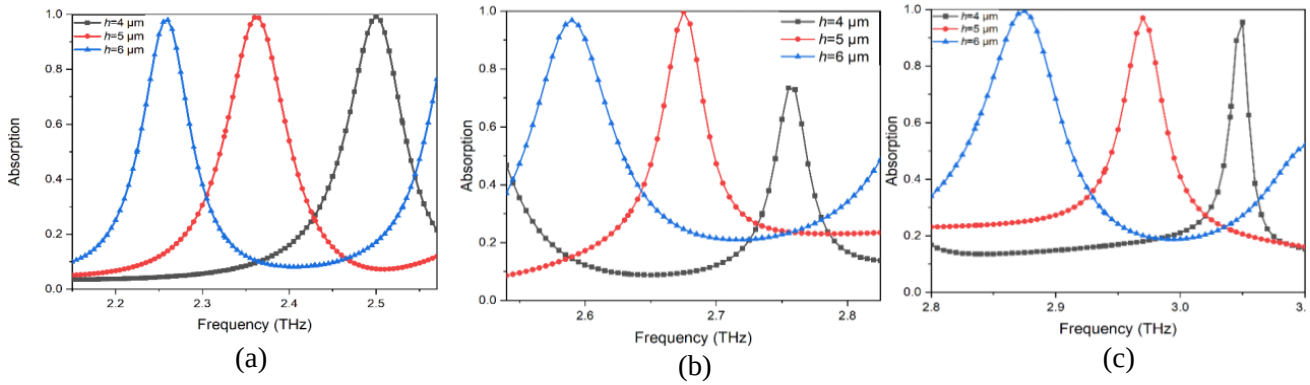

Figure 6. Parametric sweep for substrate thickness at (a) 2.36 THz, (b) 2.675 THz, (c) 2.97 THz.

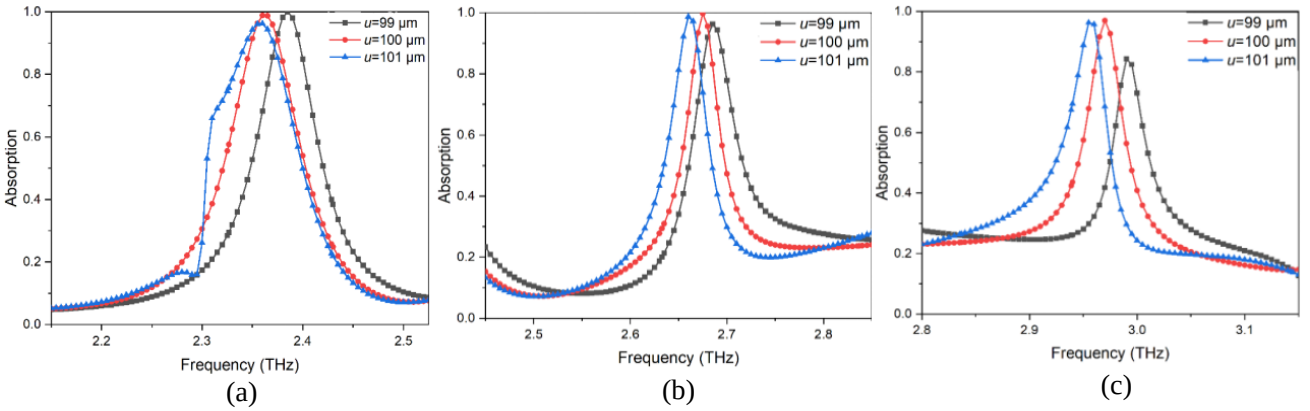

Figure 7. Parametric sweep for unit cell dimension at (a) 2.36 THz, (b) 2.675 THz, (c) 2.97 THz.

Q-factor, is obtained at a height of 5 μm. In Fig. 6(b), it is seen that the optimal peak is obtained for $h = 5$ μm, increasing or decreasing the height, reduces the absorption. Similarly, Fig. 6(c) denotes that for $h = 5$ μm, the best results are achieved in terms of both the bandwidth and peak absorption. The wave absorption happens when the impedance of the absorber matches that of the free space or 377 Ω. The impedance matching depends on the substrate thickness, and for a thickness of 5 μm the impedance is close to that of the free space, resulting in wave absorption for all the three bands. Fig. 7 represents the parametric sweep for dimension of the unit cell (u). Again, when the unit cell dimension rises, the resonant frequency drops and vice versa. In terms of peak absorption and FWHM, $u = 100$ μm provides the best absorption properties in all three bands, as shown in Fig. 7. The effective permittivity and effective permeability of the structure depend on the unit cell dimension. Fig. 8 shows the parametric survey for the radius r of the CPRs. When the radii of the CPRs are increased, the resonance shifts to a lower frequency. When the radii of the CPRs are decreased, the resonance frequency shifts to a higher frequency. The best absorption characteristics are achieved for $r = 13$ μm and on enlarging or diminishing the radius further, either the absorption decreases, or there is a significant increase in the value of FWHM, thus indicating a lower Q-factor which is not at all desired.

It is quite obvious that in practical applications the light wave is more obliquely incident upon the absorber rather than normal incidence. Hence, it is much required to study the absorption characteristics of the absorber under different angles of incidence. The frequency-reliant absorption spectra for various angles of incidence are depicted in Fig. 9 for all the three resonant frequencies. It clearly shows a decent performance of the proposed metamaterial absorber for quite a wide range of angle of incidence. The minor shifts in the absorption peaks can also be observed, which occurs due to variations in the angle of incidence from 0° to 60° at a step size of 15°. Thus the sensor maintains a nice absorption stability

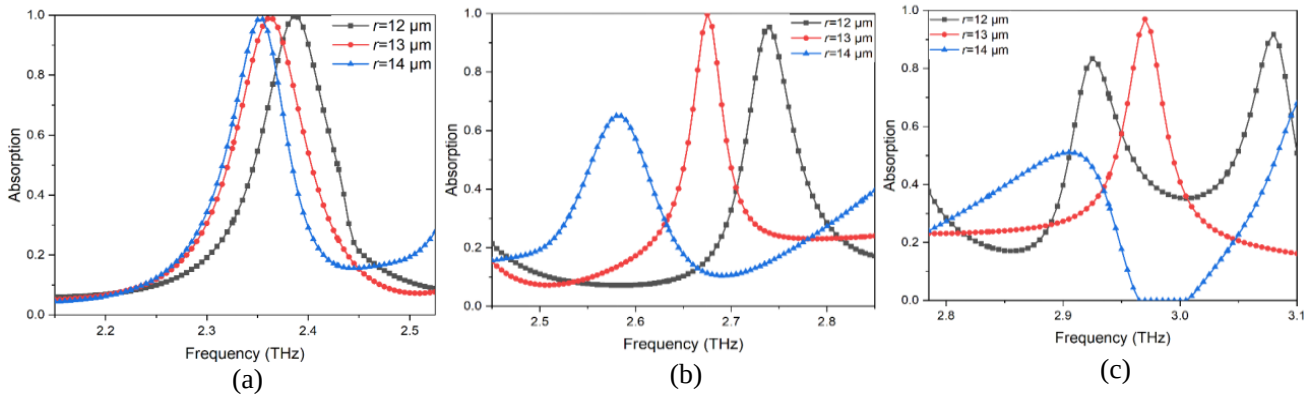

Figure 8. Parametric sweep for radius of CRRs at (a) 2.36 THz, (b) 2.675 THz, (c) 2.97 THz.

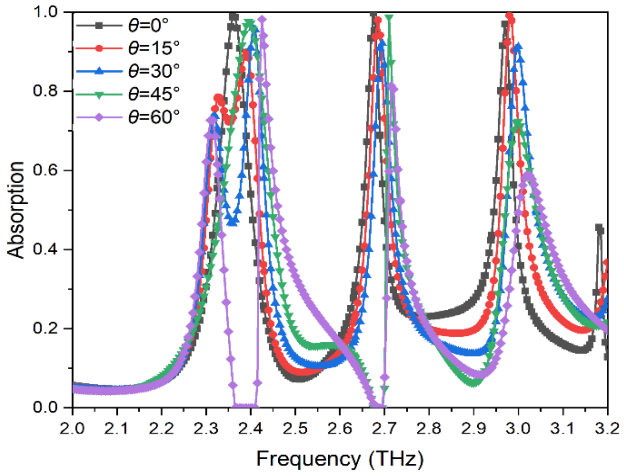

Figure 9. Parametric analysis for different angle of incidence at 2.36 THz, 2.675 THz, 2.97 THz.

Table 2. Peak absorption varies with refractive index.

Refractive Index (n)	1	1.02	1.04	1.06	1.08
Band 1 absorption	98.84	97.9	96.5	97.9	97.1
Band 2 absorption	99.77	98.99	99.92	99.65	96.53
Band 3 absorption	97.0	99.7	99.78	93.60	89.44

for a broad range of incident angles.

The changes in the absorption spectrum due to change in the refractive index of the encompassing medium has been depicted in Fig. 10 for 2.36 THz, 2.675 THz, and 2.97 THz, respectively, where it is clearly observed that on increasing the refractive index, the resonant frequency decreases and vice-versa. The refractive index has been adjusted at intervals of 0.02 from $n = 1.00$ to $n = 1.08$. The refractive index in this region was chosen because it may be employed for gas sensing applications [19]. It can also be shown that for a little change in the refractive index of the surrounding medium, there is a significant shift in the peaks of the absorption spectrum, demonstrating that the suggested design works well as a refractive index sensor. Table 2 also provides justification for the sensor's quality, where it is found that the absorption percentage of the peaks barely goes below 90%, and Table 3 as well, where the

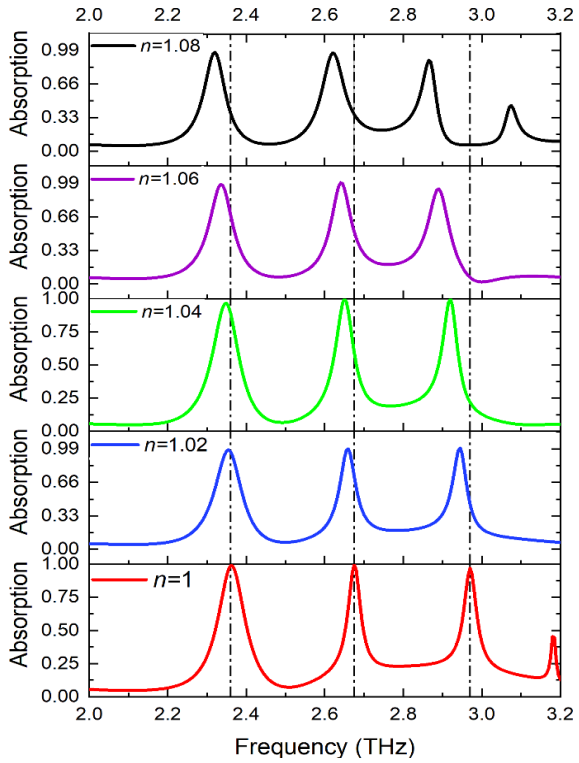

Figure 10. Absorption spectra for different refractive index.

Table 3. Resonance frequency in THz, FWHM and Q factor at different refractive indices.

		Refractive Index (n)				
		1	1.02	1.04	1.06	1.08
Band 1	Resonance Frequency (THz)	2.36	2.35	2.34	2.33	2.34
	FWHM	0.08	0.08	0.08	0.06	0.06
	Q factor	29.5	29.37	29.25	38.83	39.0
Band 2	Resonance Frequency (THz)	2.675	2.660	2.649	2.6403	2.645
	FWHM	0.04	0.05	0.05	0.06	0.06
	Q factor	66.8	53.2	52.98	44.0	44.08
Band 3	Resonance Frequency (THz)	2.97	2.944	2.919	2.888	2.86
	FWHM	0.05	0.05	0.05	0.06	0.07
	Q factor	59.4	58.88	58.38	48.13	40.85

FWHMs of the peaks range between 0.04 and 0.08 THz which is very narrow and hence, preferred for sensing applications. The absorption characteristics change with the change in the refractive index of the surrounding medium, which results in variation in the peak absorption and in the Q-factor.

The sensitivity plots for the various absorption bands are shown in Fig. 11. The following equations describe the correlation between the resonant frequency and the refractive index of the enclosing medium which is generally linear and can be given by the following equations.

$$f_1 = 2.90104 - 0.5401n \quad (2)$$

$$f_2 = 3.3752 - 0.701n \quad (3)$$

$$f_3 = 4.481 - 1.5025n \quad (4)$$

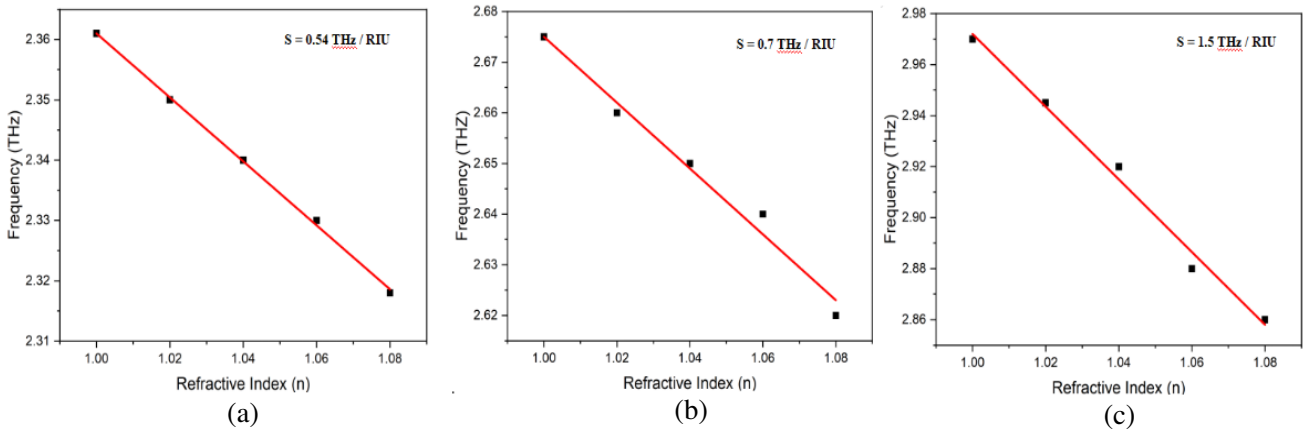

Figure 11. In three absorption bands, the resonance frequency is shown against the refractive index. (a) Band 1, (b) Band 2, (c) Band 3.

where f_1, f_2, and f_3 are the resonance frequencies in band 1, band 2, and band 3 plots. The sensitivity of the first band is 0.54 THz/RIU, and its Figure of Merit (FoM) is 6.75. FoM is the ratio of sensitivity and the FWHM. For band 2, the sensitivity is 0.70 THz/RIU, and the FoM is 17.5. For the last band the sensitivity is 1.5 THz/RIU, and its FoM is 30. As a result, the suggested refractive index sensor has excellent sensitivity and FoM in all of its absorption bands.

4. CONCLUSION

In recent years, on account of their impressive sensing and detecting performance in terahertz regime, metamaterial absorber has attracted wide attention and eventually developed into a field of interest for the researchers. This paper proposes a one-of-a-kind design of metamaterial absorber, having adjoining rectangular patches in the form of a Plus symbol along with four identical CPRs on the upper plane of a Gallium Arsenide (GaAs) substrate. Because of the lateral displacement of the absorption peaks caused by changes in the refractive index of the surrounding medium, it is an outstanding refractive index sensor. The sensor has absorption rates of 99.0%, 99.75%, and 98.0% at three different resonant frequencies of 2.36 THz, 2.675 THz, and 2.97 THz, respectively, with a narrow FWHM of 0.08, 0.04, and 0.05 THz, which results in a Q-factor of 29.5, 66.8, and 59.4 correspondingly. The design's sensitivities are 0.54 THz/RIU, 0.7 THz/RIU, and 1.5 THz/RIU in the three distinct absorption peaks with a corresponding FoM of 6.75, 17.5, and 30, respectively. The multi-band sensor can be used for sensing applications.

Funding: This is not relevant. (NA)

Conflict of interests/Competing Interests: The authors state that they do not have any conflicts of interest.

Availability of data and material: NA (Not applicable)

Code availability: This does not apply.

Authors' Contributions: The author devised the concept, developed and simulated the structure, acquired the data, and composed the paper.

Ethics Approval: This is not relevant.

Consent to Participate: The author expresses his willingness to join.

Consent for publication: The author consents to the publication of his work.

REFERENCES

1. Shamonina, E. and L. Solymar, "Metamaterials: How the subject started," *Metamaterials*, Vol. 1, 12–18, 2007.
2. Ramakrishna, S. A. and T. M. Grzegorczyk, *Physics and Application of Negative Refractive Index Materials*, CRC Press, Boca Raton, 2008.
3. Ali, H. O., A. M. Al-Hindawi, Y. I. Abdulkarim, E. Nugoolcharoenlap, T. Tippo, F. Alkurt, O. Altıntaş, and M. Karaaslan, "Simulated and experimental studies of multi-band symmetric metamaterial absorber with polarization independent for radar applications," *Chinese Physics B*, 1674–1056, 2021.
4. Abdulkarim, Y. I., Ş. Dalgaç, F. O. Alkurt, et al., "Utilization of a triple hexagonal split ring resonator (SRR) based metamaterial sensor for the improved detection of fuel adulteration," *J. Mater Sci.: Mater Electron.*, Vol. 32, 24258–24272, 2021.
5. Dalgaç, Ş., F. Karadağ, M. Bakır, O. Akgöl, E. Ünal, and M. Karaaslan, "Chiral metamaterial-based sensor applications to determine quality of car lubrication oil," *Transactions of the Institute of Measurement and Control*, Vol. 43, No. 7, 1640–1649, 2021.
6. Pelluri, R. and B. Appasani, "Genetic algorithm optimized X-band absorber using metamaterials," *Progress In Electromagnetics Research Letters*, Vol. 69, 59–64, 2017.
7. Verma, V. K., et al., "An octaband polarization insensitive terahertz metamaterial absorber using orthogonal elliptical ring resonators," *Plasmonics*, Vol. 15, No. 1, 75–81, 2020.
8. Appasani, B., et al., "A simple multi-band metamaterial absorber with combined polarization sensitive and polarization insensitive characteristics for terahertz applications," *Plasmonics*, Vol. 14, 737–742, 2019.
9. Ling, X. Y., Z. Y. Xiao, and X. X. Zheng, "Tunable terahertz metamaterial absorber and the sensing application," *J. J. Mater. Sci. Mater. Electron.*, Vol. 29, No. 1, 1–7, 2017.
10. Appasani, B., "An octaband temperature tunable terahertz metamaterial absorber using tapered triangular structures," *Progress In Electromagnetics Research Letters*, Vol. 95, 9–16, 2021.
11. Tao, H., et al., "Performance enhancement of terahertz metamaterials on ultrathin substrates for sensing applications," *Applied Physics Letters*, Vol. 97, No. 26, 2010.
12. Appasani, B., "Temperature tunable seven band terahertz metamaterial absorber using slotted flower-shaped resonator on an InSb substrate," *Plasmonics*, 1–7, 2021.
13. Cong, L. and R. Singh, "Sensing with THz metamaterial absorbers," 2014, arXiv:1408.3711. [Online]. Available: https://arxiv.org/abs/1408.3711.
14. Mirzaei, S., N. G. Green, M. Rotaru, and S. H. Pu, "Detecting and identifying DNA via the THz backbone frequency using a metamaterial based label-free biosensor," *Proceedings of SPIE*, Vol. 10103, 2017.
15. Saadeldin, A. S., M. F. O. Hameed, E. M. A. Elkaramany, and S. S. A. Obayya, "Highly sensitive terahertz metamaterial sensor," *IEEE Sensors Journal*, Vol. 19, No. 18, 7993–7999, Sept. 15, 2019.
16. Banerjee, S., U. Nath, P. Dutta, A. V. Jha, B. Appasani, and N. Bizon, "A theoretical terahertz metamaterial absorber structure with a high quality factor using two circular ring resonators for biomedical sensing," *Inventions*, Vol. 6, No. 4, 78, 2021.
17. Shen, F., J. Qin, and Z. Han, "Planar antenna array as a highly sensitive terahertz sensor," *Applied Optics*, Vol. 58, 540, 2019.
18. Li, Y., X. Chen, F. Hu, D. Li, H. Teng, Q. Rong, W. Zhang, J. Han, and H. Liang, "Four resonators based high sensitive terahertz metamaterial biosensor used for measuring concentration of protein," *Journal of Applied Physics D*, Vol. 52, 95–105, 2019.
19. Xiang, Y., J. Zhu, L. Wu, Q. You, B. Ruan, and X. Dai, "Highly sensitive terahertz gas sensor based on surface plasmon resonance with graphene," *IEEE Photonics Journal*, Vol. 10, No. 1, 1–7, Feb. 2018, Art no. 6800507, doi: 10.1109/JPHOT.2017.2778245.
20. Banerjee, S., et al., "A terahertz metamaterial absorber based refractive index sensor with high quality factor," *2021 13th International Conference on Electronics, Computers and Artificial*

Intelligence (ECAI), 1–4, 2021, doi: 10.1109/ECAI52376.2021.9515149.

21. Nickpay, M. R., M. Danaie, and A. Shahzadi, "Highly sensitive THz refractive index sensor based on folded split-ring metamaterial graphene resonators plasmonics," *Plasmonics*, 2021.
22. Yahiaoui, R., S. Tan, L. Cong, R. Singh, F. Yan, and W. Zhang, "Multispectral terahertz sensing with highly flexible ultrathin metamaterial absorber," *Journal of Physics D: Applied Physics*, Vol. 118, 83–103, 2015.
23. Zhang, W., J.-Y. Li, and J. Xie, "High sensitivity refractive index sensor based on metamaterial absorber," *Progress In Electromagnetics Research M*, Vol. 71, 107–115, 2018.
24. Yan, Z., C. Tang, G. Wu, Y. Tang, P. Gu, J. Chen, Z. Liu, and Z. Huang, "Perfect absorption and refractive-index sensing by metasurfaces composed of cross-shaped hole arrays in metal substrate," *Nanomaterials*, Vol. 11, 63, 2021, https://doi.org/10.3390/nano11010063.
25. Xie, Q., G. X. Dong, B. X. Wang, and W. Q. Huang, "High-Q fano resonance in terahertz frequency based on an asymmetric metamaterial resonator," *Nanoscale Resonance Letters*, Vol. 13, 294, 2018.
26. Zhang, W., et al., "Ultrasensitive dual-band terahertz sensing with metamaterial perfect absorber," *2017 IEEE MTT-S International Microwave Workshop Series on Advanced Materials and Processes for RF and THz Applications (IMWS-AMP)*, 1–3, 2017, doi: 10.1109/IMWS-AMP.2017.8247404.
27. Zhu, L., H. Li, L. Dong, W. Zhou, M. Rong, X. Zhang, and J. Guo, "Dual-band electromagnetically induced transparency (EIT) terahertz metamaterial sensor," *Opt. Mater. Express*, Vol. 11, 2109–2121, 2021.
28. Lan, F., et al., "Dual-band refractometric terahertz biosensing with intensewave-matter-overlap microfluidic channel," *Biomed. Opt. Exp.*, Vol. 10, No. 8, 3789–3799, 2019.
29. Wang, J., T. Lang, Z. Hong, M. Xiao, and J. Yu, "Design and fabrication of a triple-band terahertz metamaterial absorber," *Nanomaterials*, Vol. 11, No. 5, 1110, 2021.
30. Li, Z., Z. Yi, T. Liu, L. Liu, X. Chen, F. Zheng, J. Zhang, H. Li, P. Wu, and P. Yan, "Three-band perfect absorber with high refractive index sensing based on an active tunable Dirac semimetal," *Physical Chemistry Chemical Physics*, Vol. 23, No. 32, 17374–17381, 2021.
31. Wang, B. X., G. Z. Wang, and T. Sang, "Simple design of novel triple-band terahertz metamaterial absorber for sensing application," *Journal of Physics D: Applied Physics*, Vol. 49, No. 16, 165307, 2016.
32. Liu, N., et al., "Plasmonic analogue of electromagnetically induced transparency at the Drude damping limit," *Nature Matter*, Vol. 8, 758–762, 2009.